Identifying Atmospheric River Reconnaissance Targets Using Ensemble Forecasts

Travis J. Elless[1*], Xingren Wu[1], and Vijay Tallapragada[2]
[1]I.M. Systems Group at NOAA/NWS/NCEP/EMC [2]NOAA/NWS/NCEP/EMC
[*]travis.j.elless@noaa.gov

1. Introduction

Model forecasts exhibiting large variability are a detriment to a forecaster's confidence. This can be extremely problematic for large-impact weather events, such as precipitation forecasts in the drought prone Western United States. The Atmospheric River (AR) Reconnaissance field campaign (Ralph *et al*. 2020) provides additional observations in upstream regions/features exhibiting high ensemble forecast variability, with the goal of reducing short-range West Coast precipitation forecast uncertainty. Due to time constraints, mission planning generally uses 00 UTC forecasts to assess variability in the 60-84-h precipitation forecasts and subsequently identify sensitive areas (targets) in model fields at 48 h. Since 2019, the Environmental Modeling Center (EMC) has developed tools to provide potential mission targets to the field campaign, based on ensemble sensitives calculated from a combined 21-member (upgraded to 31-member in 2021) Global Ensemble Forecast System and 21-member Canadian Ensemble Prediction System super ensemble. This report highlights the methodology used for this tool, and provides example outputs that forecasters utilize.

2. EMC ensemble sensitivity tool

The EMC ensemble sensitivity tool utilizes a composite difference approach to identify upstream sensitive regions that are linked to West Coast precipitation forecast variability. Composite differences have been previously used to identify processes and features associated with large ensemble variability in forecast tropical cyclone (TC) position (Torn *et al*. 2015), TC intensity (Rios-Berrios *et al.* 2016), midlatitude cyclone intensity (Lamberson *et al*. 2016), and 500-hPa height errors (Magnusson 2017). Utilizing composite differences for this particular task first requires the identification of subsets of ensemble members based on the 60-84-h West Coast precipitation forecasts. For a given forecast, the standard deviation (SD) in accumulated precipitation is calculated for each grid point and the location with the maximum value is identified. All adjacent grid points within 66% of this maximum SD value are then identified, and precipitation amounts are averaged over this area. Figure 1 provides an example of this identification for a forecast initialized 00 UTC 20 Feb 2021. This averaging allows for sensitivity impacts to be representative of a larger geographical area, instead of focusing on individual grid point values. Ranking the area-averaged precipitation allows the creation of two subsets consisting of the 10 most/least precipitating ensemble members.

For this project, differences between these two subsets at 48 h are evaluated at each individual grid point via

$$\Delta x_i = \frac{\bar{x}_i^{Highest} - \bar{x}_i^{Lowest}}{\sigma_{x_i}}, \tag{1}$$

where Δx_i represents the composite difference for a given state variable (this field project primarily utilizes integrated vapor transport (IVT), 850-hPa equivalent potential temperature (θ_e), and 500-hPa potential vorticity), which is used as a measure of ensemble sensitivity, $x_i^{Highest}$ (x_i^{Lowest}) is the subset mean for the given state variable, and σ_{xi} is the SD of the state variable utilizing all ensemble members. Normalizing the difference by the SD allows for a direct comparison to be made between different model variables and levels to determine fields that are the most sensitive. Differences are found to be statistically significant at the 95% confidence interval from a 1000 iteration bootstrap resampling without replacement process; statistical significance was calculated similarly to Rios-Berrios *et al.* (2016). Figure 2 shows an example of the 48-h composite difference evaluation of 850-hPa θ_e for the 00 UTC 20 Feb 2021 initialization. Differences are primarily found on the periphery of a thermal ridge, suggesting the precipitation variability found in Washington is sensitive to the position of this ridge, such that a more meridionally oriented ridge is associated with increased precipitation in Washington; this feature was subsequently deemed a viable target for additional observations.

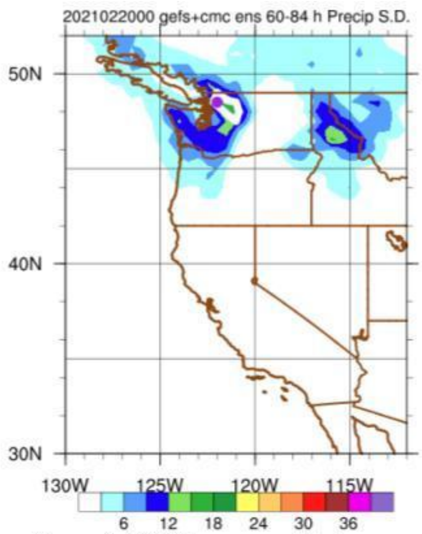

Figure 1. 60-84-h accumulated precipitation standard deviation (color fill; units mm), grid point of maximum standard deviation (purple dot), and area bound by 66% of maximum standard deviation (white line)

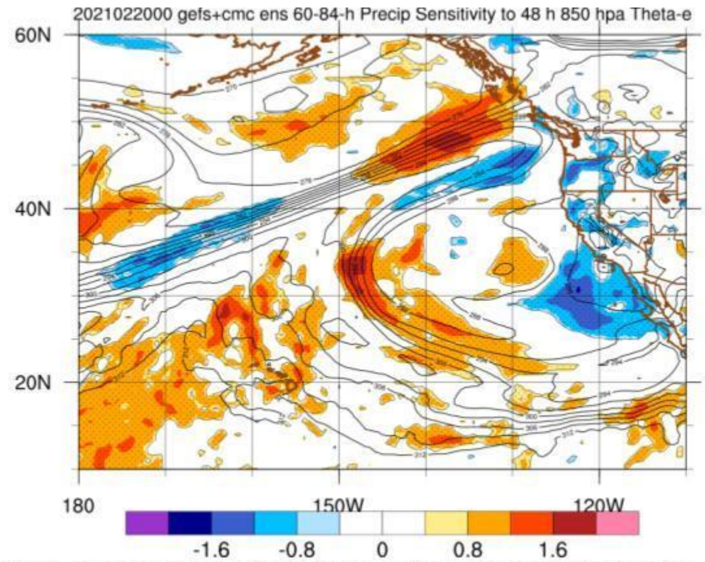

Figure 2. Ensemble mean 48-h 850-hPa equivalent potential temperature (contours) and composite difference between high and low subsets defined for the region in Fig. 1 (color fill; units standard deviation). All differences shown are statistically significant at the 95% confidence interval

3. Other applications

This methodology can be adapted to test the sensitivity of any given metric to any model field, and is a vital tool in understanding processes leading to ensemble variability. For example, this project has also identified targets using subsets created from IVT and mean sea level pressure variability. Future work includes identifying subsets from principal components of precipitation empirical orthogonal function (EOF) analysis, and utilizing this tool to identify sensitive areas associated with operational dropout events.

References

Lamberson, W. S., R. D. Torn, L. F. Bosart, and L. Magnusson, 2016: Diagnosis of the source and evolution of medium-range forecast errors for extratropical cyclone Joachim. *Wea. Forecasting,* **31,** 1197-1214.

Magnusson, L., 2017: Diagnostic methods for understanding the origin of forecast errors. *Quart. J. Roy. Meteor. Soc.,* **143,** 2129-2142.

Ralph, F. M., and Coauthors, 2020: West Coast forecast challenges and development of atmospheric river reconnaissance. *Bull. Amer. Meteor. Soc.,* **101,** E1357-E1377.

Rios-Berrios, R., R. D. Torn, and C. A. Davis, 2016: An ensemble approach to investigate tropical cyclone intensification in sheared environments. Part I: Katia (2011). *J. Atmos. Sci.,* **73,** 71-93.

Torn, R. D., J. S. Whitaker, P. Pegion, T. M. Hamill, and G. J. Hakim, 2015: Diagnosis of the source of GFS medium-range track errors in Hurricane Sandy (2012). *Mon. Wea. Rev.,* **143,** 132-152.